Phys. Med. Biol. **45** (2000) 1913–1922. Printed in the UK PII: S0031-9155(00)08486-4

Combining two excitation wavelengths for pulsed photothermal profiling of hypervascular lesions in human skin

Boris Majaron†‡⁺, Wim Verkruysse†, B Samuel Tanenbaum§, Thomas E Milner‖, Sergey A Telenkov‖, Dennis M Goodman¶ and J Stuart Nelson†

† Beckman Laser Institute and Medical Clinic, University of California, 1002 Health Sciences Road East, Irvine, CA 92612-1475, USA
‡ Jožef Stefan Institute, Jamova 39, SI-1000 Ljubljana, Slovenia
§ Department of Engineering, Harvey Mudd College, Claremont, CA 91711, USA
‖ Department of Electrical and Computer Engineering and the Biomedical Engineering Program, University of Texas, Austin, TX 78712, USA
¶ Lawrence Livermore National Laboratory, University of California, Livermore, CA 94550, USA

E-mail: majaron@bli.uci.edu

Received 7 October 1999, in final form 24 March 2000

Abstract. When pulsed photothermal radiometry (PPTR) is used for depth profiling of hypervascular lesions in human skin, melanin absorption also heats the most superficial skin layer (epidermis). Determination of lesion depth may be difficult when it lies close to the epidermal–dermal junction, due to PPTR's limited spatial resolution. To overcome this problem, we have developed an approximation technique, which uses two excitation wavelengths (585 and 600 nm) to separate the vascular and epidermal components of the PPTR signal. This technique permits a noninvasive determination of lesion depth and epidermal thickness *in vivo*, even when the two layers are in close physical proximity to each other. Such information provides the physician with guidance in selecting the optimal parameters for laser therapy on an individual patient basis.

1. Introduction

Time-resolved measurement of infrared (IR) radiant emission following pulsed laser irradiation, known as pulsed photothermal radiometry (PPTR), can be used to assess the longitudinal temperature profile induced in a layered sample (Tam and Sullivan 1983). Knowing the absorption properties of the sample chromophores, their depth distribution may then be determined (Long *et al* 1987, Crostack *et al* 1989). Such a PPTR technique was recently introduced for *in vivo* depth profiling of hypervascular lesions in human skin, such as port-wine stain (PWS) birthmarks (Jacques *et al* 1993, Milner *et al* 1995).

PWS consists of an excess of ectatic blood vessels, usually fully contained within the most superficial millimetre of the dermis. PWS depth varies on an individual patient basis, but on average, the highest fractional blood content is found between 200 and 400 μm below the epidermal–dermal junction (Barsky *et al* 1980).

The ability of PPTR to correctly determine the depth of sub-surface chromophores in turbid media has been demonstrated previously by profiling layered tissue phantoms (Vitkin

⁺ Correspondence to Dr Boris Majaron, Beckman Laser Institute and Medical Clinic.

0031-9155/00/071913+10$30.00

et al 1995, Milner *et al* 1996), and comparison with histological assessment of PWS depths (Milner *et al* 1996). However, when a visible laser pulse is used to increase the temperature of PWS blood vessels for the purpose of PPTR profiling *in vivo*, melanin absorption heats also the epidermis (50–150 μm thick superficial layer of skin). When the PWS lies in close proximity to the epidermis, determination of lesion depth may be difficult due to the inherently limited spatial resolution of PPTR (Milner *et al* 1995, Smithies *et al* 1998). To overcome this problem, we present an approximation technique that achieves improved selectivity by utilizing two excitation wavelengths. Such an approach enables *in vivo* determination of both PWS depth and epidermal thickness, which is required for optimization of laser therapy involving cryogen spray cooling on an individual patient basis (Anvari *et al* 1995a, b, Verkruysse *et al* 2000).

2. Method

2.1. Experimental setup and theory

A PWS lesion on the arm of a volunteer patient was irradiated with two 1.5 ms duration pulses at 585 and 600 nm, delivered sequentially from a ScleroPLUS pulsed dye laser (Candela, Wayland, MA). At both wavelengths, the energy density at the centre of a 6 mm diameter laser spot was approximately 5 J cm^{-2}. The transient increase in IR radiant emission from the central 1.9 × 1.9 mm^2 area was recorded with an InSb focal-plane-array camera (Raytheon, Dallas, TX; detection band 3–5 μm) at a rate of 200 frames per second. After calibrating the response of the 64 × 64 array detector elements with a temperature stabilized blackbody, averaging over the array and subtracting the radiant emission level before the pulsed laser exposure, signals $s_{585}(t)$ and $s_{600}(t)$ were obtained (figure 1). These signals represent the radiometric temperature increase induced by pulsed exposure at 585 and 600 nm, respectively. The radiometric temperatures are given in degrees Celsius of the blackbody temperature increase. (Note, however, that they do *not* represent the skin surface temperature, due to the finite penetration depth of the detected IR radiation.)

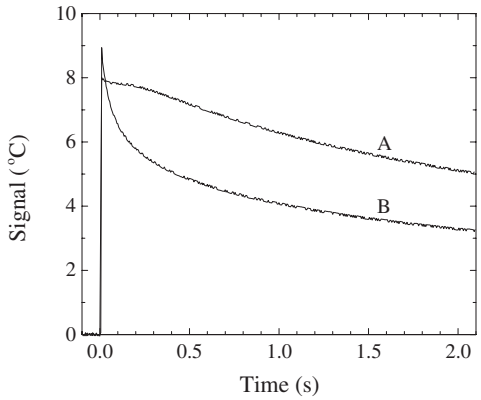

Figure 1. PPTR signals obtained from the same spot in a PWS lesion *in vivo* using excitation wavelengths of 585 nm (curve A), and 600 nm (B).

Reconstruction of the initial temperature profile from the PPTR signals is a severely ill posed inverse problem (Milner *et al* 1995, Prahl 1996). In our case, it is solved by a dedicated iterative algorithm using a nonnegative-constrained conjugate-gradient method (Milner *et al* 1995). As an example, consider the longitudinal temperature profile immediately after 585 nm

excitation computed from signal $s_{585}(t)$ (figure 1), presented in figure 2(a). The three curves shown are iterative solutions, obtained with different degrees of regularization. In accordance with the discrepancy principle (Groetsch 1984), the iterative algorithm runs until the Euclidian norm of the residue reaches a level defined by a preset signal-to-error ratio (SER). At low values of SER, we obtain under-iterated solutions, which are blurred images of the actual temperature profile. By increasing SER, near optimal solutions that show more detail are obtained, eventually followed by over-iterated results. As discussed previously by Milner *et al* (1995), the latter often oscillate, as the algorithm attempts to fit mismatches between the experimental and theoretically predicted signals (dotted line). In this study, we avoid the issue of optimal regularization by presenting a series of iterative solutions for each example discussed. Since at high SER settings (SER = 50 in figures 2(a), (b)) the above criterion for terminating the iteration cannot be met, the iteration run is stopped after an arbitrarily chosen high number of iteration steps ($n = 100$, compared to $n = 6$ reached at SER = 30). Clearly, in the presented example, the temperature profile in the PWS layer cannot be resolved from the heated epidermis.

2.2. *Combining two excitation wavelengths*

The calibrated PPTR signals $s(t)$ are linear functions of the longitudinal temperature distribution immediately following pulsed laser exposure (Milner *et al* 1995). Therefore, the superposition principle can be applied to express signal $s_{585}(t)$ as a sum of two signal components, originating from the heated PWS ($x(t)$), and epidermis ($y(t)$):

$$s_{585}(t) = x(t) + y(t). \tag{1}$$

At 600 nm, the absorption and scattering properties of the epidermis and dermis are essentially equivalent to those at 585 nm (Wan *et al* 1981). As a result, the temperature profile in the epidermis and, consequently, the corresponding signal component, are nearly equal at both excitation wavelengths. In contrast, absorption by blood is significantly weaker at 600 nm than at 585 nm (van Kampen and Zijlstra 1965; see table 1). This results in a smaller contribution from the PWS to the PPTR signal obtained with 600 nm excitation. The latter can therefore be approximated by

$$s_{600}(t) = \alpha x(t) + \beta y(t) \tag{2}$$

α and β are unknown positive constants. Based on the above described spectral properties of the tissue components, we expect their values to be $\alpha < 1$ and $\beta \approx 1$.

Table 1. Absorption coefficients of oxygenated and deoxygenated human blood (hematocrit 40) at 585 nm, 600 nm, and the ratio of the two (from van Kampen and Zijlstra 1965).

Oxygenation level (%)	μ(585 nm) (mm^{-1})	μ(600 nm) (mm^{-1})	μ(600 nm)/μ(585 nm)
100	18.0 ± 0.9	2.0 ± 0.2	0.11 ± 0.02
0	16.9 ± 0.6	7.0 ± 0.3	0.41 ± 0.03

Due to the difference in blood absorption, 600 nm laser radiation may penetrate deeper into the PWS compared to 585 nm. Consequently, the PWS temperature profiles induced by the 600 and 585 nm laser pulses are in general not exactly proportional. Nevertheless, the proportionality assumed in equation (2) is valid at least in a thin top layer of the PWS, where both temperature profiles can be linearized. The first-order approximation made in equation (2) is thus appropriate for reconstruction of the epidermal profile and top boundary of the PWS,

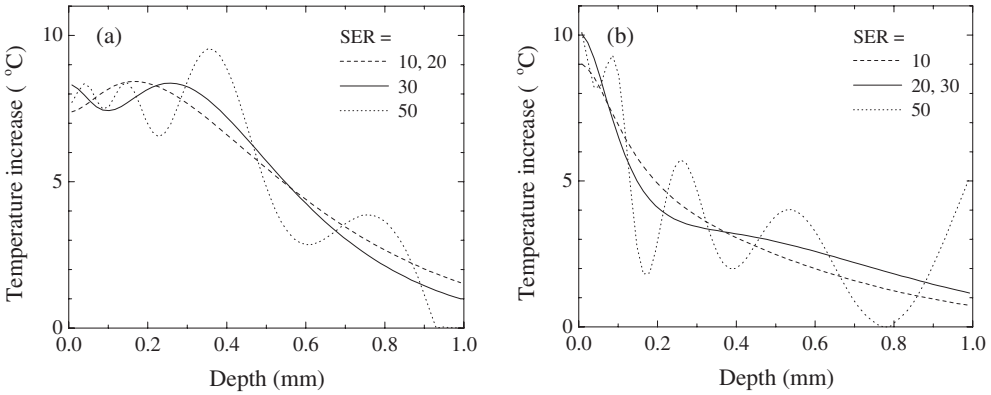

Figure 2. Longitudinal temperature profiles immediately after pulsed laser exposure, as reconstructed from PPTR signals in figure 1 using the inversion algorithm. The three curves shown for each example are iterative solutions obtained with different degrees of regularization (see text). (a) Excitation wavelength 585 nm, (b) excitation wavelength 600 nm.

as required for optimization of therapy, but can be expected to deteriorate at deeper depths. We discuss the limitations of such an approach in more detail in section 4.

From equations (1) and (2), the PWS and epidermal components of $s_{585}(t)$ can be derived as:

$$x(t) = \frac{\beta s_{585}(t) - s_{600}(t)}{(\beta - \alpha)} \tag{3a}$$

$$y(t) = \frac{s_{600}(t) - \alpha s_{585}(t)}{(\beta - \alpha)}. \tag{3b}$$

By applying our reconstruction algorithm to each of these components separately, the initial temperature profiles in the PWS and epidermis can be obtained independently. Since the values of α and β are not known, we estimate them as follows.

First, we use the fact that the radiometric signal immediately following pulsed laser exposure results predominantly from the temperature rise within a few penetration depths of the detected IR radiation (40–50 μm) from the skin surface. Since the blood vessels are located deeper (>100 μm) in the skin, we require that the PWS signal component starts from $x(t = 0) = 0$, yielding $\beta = s_{600}(t = 0)/s_{585}(t = 0)$. A signal, proportional to the PWS contribution $x(t)$, can then be calculated as $\beta s_{585}(t) - s_{600}(t)$ (see equation (3*a*)). The temperature profile reconstructed therefrom is proportional to the temperature increase in the PWS induced by 585 nm excitation.

Second, we know that reconstruction of a pure epidermal component should not contain any temperature increase deeper than 200 μm below the skin surface. Therefore, we calculate signals $y(t)$ according to equation (3*b*) with increasing values of α, starting from 0, and reconstruct the corresponding temperature profile from each of these signals. This is repeated until the temperature increase deeper than 200 μm below the skin surface drops to zero. The value of α at which this happens is taken as the best estimate, and is used to normalize the amplitude of the previously obtained PWS temperature profile (by simply dividing it by $(\beta - \alpha)$, in accordance with equation (3*a*)).

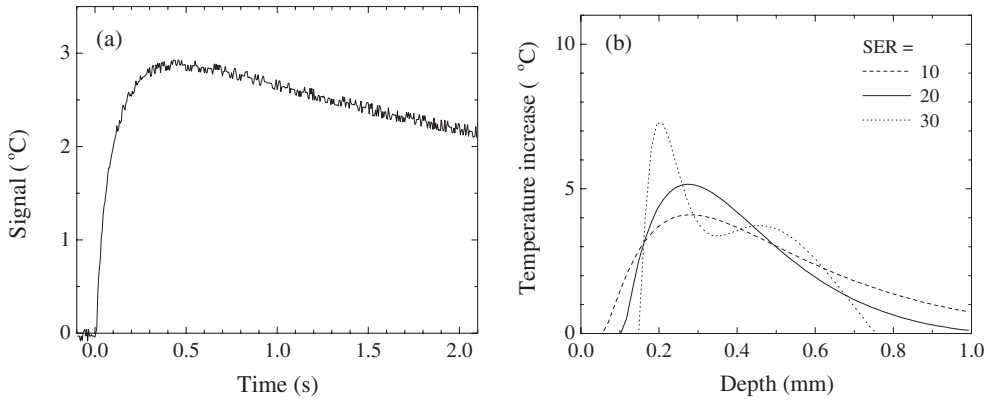

Figure 3. (a) PPTR signal proportional to the PWS contribution x(t), calculated from experimental signals in figure 1 (as $\beta s_{585}(t) - s_{600}(t)$). (b) Non-normalized temperature profile in the PWS, as calculated from the signal in figure 3(a).

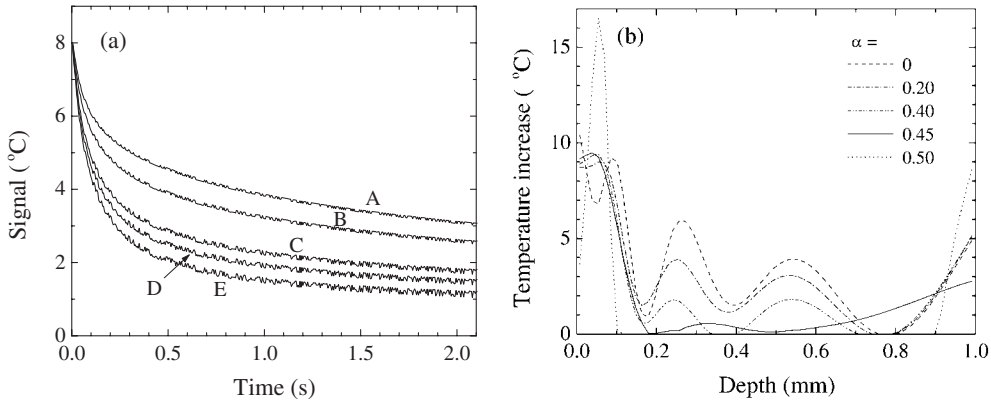

Figure 4. (a) PPTR signals $y(t)$, calculated from signals in figure 1 using equation (3*b*) with increasing values of α: 0 (A), 0.20 (B), 0.40 (C), 0.45 (D), and 0.50 (E). (b) Temperature profiles reconstructed from these signals.

3. Results

Figures 2(a) and 2(b) present temperature profiles for a PWS birthmark *in vivo* (on a patient's forearm), as reconstructed from PPTR signals $s_{585}(t)$ and $s_{600}(t)$ in figure 1, respectively. Without knowing the actual temperature profile, it is certainly somewhat ambiguous whether the solution with SER $= 30$ (solid line) is closer to optimal than that obtained with SER $= 10$ (dashed). Irrespective of that, these results convincingly demonstrate how, in the presented example, neither the PWS depth nor epidermal thickness can be assessed by reconstruction from a single PPTR signal. In addition, they illustrate the previously discussed absorption properties of melanin and blood by indicating a similar average temperature increase in the superficial layer (epidermis, containing melanin) but considerably lower temperature rise deeper in the skin with 600 nm excitation (figure 2(b)), compared to 585 nm (figure 2(a)).

Figure 3(a) presents a signal proportional to the PWS component $x(t)$, calculated from the experimental PPTR signals as $\beta s_{585}(t) - s_{600}(t)$. As described in the previous section, the value of β is adjusted to bring the first point of this signal to 0 ($\beta = 1.06$ for the presented example).

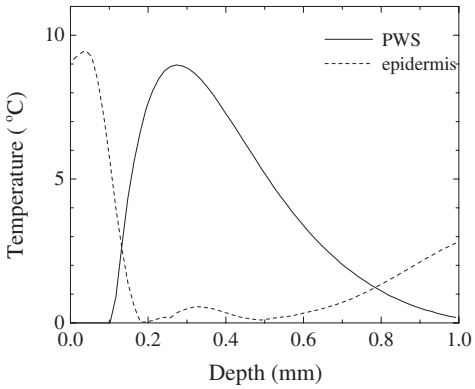

Figure 5. Initial temperature profiles in the PWS, as obtained after normalization of the result in figure 3(b) (solid line), and in the epidermis (dashed). Both solutions are correct only at depths up to 0.2 mm ($\alpha = 0.45$).

The reconstructed temperature profile (figure 3(b)) is proportional to the temperature increase in the PWS layer, and clearly shows its top boundary. The solution obtained with SER = 30 can be disregarded as over-iterated based on its oscillatory shape, which is in agreement with the lower signal-to-noise ratio in the subtracted signal (figure 3(a)) compared to the original single-wavelength PPTR signals (see figure 1). The SER = 20 solution is thus considered as the closest available estimate of the initial temperature profile (solid line).

The signals $y(t)$ calculated according to equation (3*b*) with α increasing from 0 to 0.50 (curves A–E) are presented in figure 4(a). Temperature profiles reconstructed from these signals (figure 4(b); SER = 50) show steadily decreasing temperatures at depths below 150–200 μm, with values of α increasing up to 0.40. At $\alpha = 0.45$, the PWS contribution to the temperature profile practically disappears. In the most superficial 150 μm (epidermis), the temperature profile varies little from $\alpha = 0.20$ to 0.45, indicating that this part of the solution is insensitive to small variations of α. While the PWS contribution is completely absent from the solution at $\alpha = 0.50$, the abrupt change in width and height of the epidermal profile indicate that this value is most likely too high. A further discussion on determining the best choice of α is given in section 4.

Figure 5 presents the final result, showing separately the temperature profiles in the PWS and epidermis (using $\alpha = 0.45$), which are evidently in close proximity to each other. In fact, our result indicates an overlap of the two profiles, which could result from the uneven shape of the epidermal–dermal junction, but also from broadening of one or both profiles by the limited spatial resolution of the reconstruction algorithm.

In order to establish a direct correlation between our two-wavelength approximation algorithm and single-wavelength PPTR profiling, which has been thoroughly tested before (Vitkin *et al* 1995, Milner *et al* 1996), we present in figure 6(a) a similar analysis of another PWS lesion (located on a finger of the same patient). In the PPTR signal obtained with 585 nm excitation (curve A in figure 6(a)), the initial spike, resulting from the heated superficial layer, and the delayed contribution from the deeper lying PWS can be easily distinguished. This indicates that in this specific example, the PWS vascular cluster is spatially separated from the epidermis, which is confirmed by the initial temperature profiles reconstructed from this signal (figure 6(b)). The signals in figure 6(a) also illustrate how the initial spike, resulting from epidermal heating, is reproduced in the signal obtained with 600 nm exposure (curve B), whereas the delayed contribution from subsurface PWS is considerably diminished.

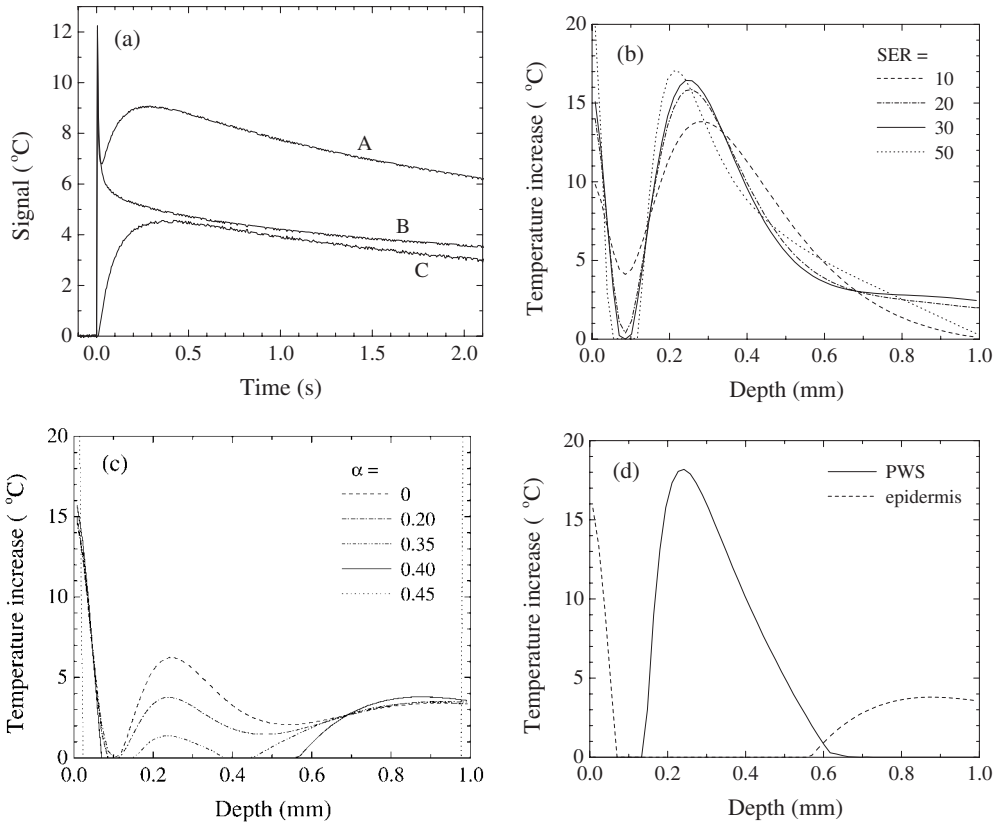

Figure 6. (a) PPTR signals $s_{585}(t)$ (curve A) and $s_{600}(t)$ (B) obtained from another PWS lesion *in vivo*, and the component proportional to the PWS contribution $x(t)$, calculated as $\beta s_{585}(t) - s_{600}(t)$ (C). (b) Longitudinal temperature profile immediately after the laser exposure, as reconstructed from signal $s_{585}(t)$ in figure 6(a). (c) Temperature profiles as reconstructed from signals $y(t)$, calculated using increasing values of α. (d) Initial temperature profiles in the PWS (solid line) and in the epidermis (dashed; $\alpha = 0.40$). The result closely matches the profile in figure 6(b) up to a depth of ∼0.40 mm.

Figure 6(c) illustrates the next step of the corresponding two-wavelength analysis in which the value of $\alpha = 0.40$ is determined. The final result of this analysis is presented in figure 6(d). The temperature profiles in the epidermis (SER = 30) as well as PWS (SER = 20) replicate very closely the ones determined by standard, single-wavelength PPTR profiling (figure 6(b)), up to a depth of ∼400 μm. The two heated layers are separated by approximately 60 μm, which enables the reconstruction algorithm to differentiate their contributions to the 585 nm signal, in contrast to the previous example (figure 2(a)).

4. Discussion

The presented method is based on the principle of superposition, which relies on the linear relationship between the PPTR signals following laser exposure $s(t > 0)$ and the induced temperature distribution $\Delta T(z, t = 0)$ (equation (5) in Milner *et al* 1995). This linearity, which is to the best of our knowledge used in all related work thus far, arises from a power series expansion of the emitted infrared radiation intensity (Planck's law) around the starting

temperature, of which only the linear term is preserved. The emitted radiation is therefore linear in the temperature distribution only for small temperature increases. For the discussed experiment, by taking into account the acquisition wavelength band of 3–5 μm and initial skin temperature of 35 °C, the actual intensity of the emitted radiation deviates from the corresponding linear approximation by 3.8% for a homogeneous temperature increase of 10 °C. It is very important to note, however, that the amplitudes of the PPTR signals used in the presented analysis have been calibrated by comparison with infrared radiation levels emitted from a homogeneously heated black body, which eliminates most, if not all, of this nonlinearity.

As previously mentioned, equation (2) is a first order approximation, which holds in the epidermis and most superficial layer of the PWS. At deeper depths, the validity of this approximation may deteriorate, depending on differences between the temperature profiles induced in the PWS with 585 versus 600 nm irradiation. The latter likely penetrates deeper into the lesion, since, according to published data on blood vessel size distribution in PWS (Barsky *et al* 1980) and absorption properties of blood (van Kampen and Zijlstra 1965), most vessels can be expected to behave as optically thin (Lucassen *et al* 1996). This is reflected in the lower PWS temperature increase observed with 600 nm, compared to 585 nm excitation (figure 2).

As a result, signal $y(t)$ calculated using equation (3*b*) in general contains some contribution from deeper blood vessels, which can be expected to show up in the reconstructed temperature profiles. The 'epidermal' profile deeper than 200 μm in figure 5, is in our opinion such an artifact of the approximation method, and should not be interpreted as a melanin-mediated temperature increase. For the same reason, the presented PWS temperature profile (reconstructed from $x(t)$ differs from the actual temperature profile induced in the PWS by 585 nm excitation at depths beyond $\sim$200 μm. The same effect can be observed by comparing the results in figures 6(b) and 6(d), which differ at depths beyond $\sim$400 μm. Nevertheless, as equation (2) is valid for shallow skin depths, down to the most superficial layer of the PWS, we can conclude that the temperature profiles reconstructed from $x(t)$ and $y(t)$ are representative for determination of PWS depth and epidermal thickness, respectively, as required to guide laser therapy.

When determining the value of α as described in section 2.2, it is instructive to monitor the behaviour of the residual norm. In the example presented in figure 4(b), increasing the value of α from 0.45 to 0.50 results in a 5% higher residual norm, supporting our conclusion that the latter value is likely too high. An overestimated value of α introduces a negative heat source at the PWS position, which cannot be accounted for by the positively constrained inversion algorithm. In the second example presented (figure 6(c)), using a value of $\alpha = 0.45$ increases the residual norm by a factor of six, compared to $\alpha = 0.40$ or 0.35, confirming the value of 0.40 as the best estimate. (In view of the inexact nature of our criteria, we made no attempt to determine α more accurately than to the closest 0.05.)

In addition, we found that by adding the integrals of the PWS and epidermal temperature profiles, the integral of the profile obtained using 585 nm excitation alone is matched within a relatively narrow error margin (3.0% for figure 5 versus 2(a); 1.0% for figure 6(d) versus 6(b), as required by energy conservation. In both examples, using a larger value of α degraded this match.

PPTR profiling of four PWS sites on the same patient yielded average values of $\bar{\alpha} = 0.41$ (standard deviation s.d. $= 0.07$), and $\bar{\beta} = 1.0$ (s.d. $= 0.1$). The latter indicates that, on the average, the epidermal contributions to the PPTR signals obtained with 585 and 600 nm excitation are nearly equal. The occasionally observed differences between the amplitudes of the initial PPTR signal jump observed with the two excitation wavelengths can be attributed in part to random variations of the excitation pulse energy. In addition, due to strong scattering in dermis, the excitation fluence in epidermis may be somewhat affected by absorption in PWS blood (Verkruysse *et al* 1993). This effect would diminish the epidermal contribution to the

PPTR signal following the 585 nm excitation with respect to 600 nm, in particular when the PWS lies close to the epidermal–dermal junction (as is the case in figure 1).

Although the ratio of PWS temperature increase with 600 versus 585 nm excitation does not depend exclusively on the blood absorption coefficients at these wavelengths, it is interesting to note that the obtained value of $\bar{\alpha}$ resembles the absorption coefficient ratio for completely deoxygenated blood ($\mu_{600}/\mu_{585} = 0.41$) as compared to fully oxygenated blood (0.11; see table 1). This may indicate the effect of PWS blood deoxygenation during laser exposure, as a result of the impaired oxygen binding capacity of heamoglobin at increased temperatures (Kelman and Nunn 1966). Note that the temperature increase in the presented one-dimensional profiles reflects the average value at a given depth, whereas temperature rises in individual blood vessels are likely several times higher.

A considerable correction to the above rough estimates of the expected values of α would result from consideration of the absorption in bloodless dermis ($\mu_D = 0.22$ mm^{-1}; Verkruysse *et al* 1993). By assuming the fractional blood content in the superficial part of the PWS equal to $f = 0.06$ (Barsky *et al* 1980), for example, the value of α would be predicted at $(f\mu_{600} + \mu_D)/(f\mu_{585} + \mu_D) = 0.26$ for completely oxygenated, and 0.52 for deoxygenated blood. However, in view of the influence of other variable factors and effects, such as distribution of vessel diameters (Lucassen *et al* 1996, Verkruysse *et al* 1997) scattering in dermis (Verkruysse *et al* 1997), and dynamical changes in the optical properties of blood (Verkruysse *et al* 1998), a much more detailed study—possibly taking into account the exact three-dimensional geometry of a specific lesion—would be required in order to draw quantitative conclusions from the experimentally determined values of α.

In conclusion, the presented technique, which combines PPTR signals obtained with two different excitation wavelengths, enables determination of epidermal thickness and PWS depth *in vivo* with an accuracy sufficient to guide laser therapy, even when the two layers are in close physical proximity to each other. A direct comparison of our approach with standard, single-wavelength PPTR profiling, shows no significant difference in the epidermal profile nor PWS depth, when the two layers are separated by $\sim$60 μm. In ongoing experiments at our institution (BLIMC), we aim at improving the accuracy of PPTR profiling by using higher acquisition rates and reduced spectral detection band (Majaron *et al* 2000). We are also correlating the temperature profiles determined using the above presented approach with information obtained from non-invasive imaging techniques, such as optical Doppler tomography (Zhao *et al* 2000a, b). However, such comparisons, as well as those involving histological evaluation of PWS, are practically limited to correlations of epidermal thickness and PWS depth, since the relation between the geometry of the lesion and the laser-induced temperature profile is complicated by the nonhomogeneous distribution of the chromophores and strong scattering of the laser radiation in skin.

Acknowledgments

A research grant from the Institute of Arthritis and Musculoskeletal and Skin Diseases (AR43419) is gratefully acknowledged, as is institutional support from the Office of Naval Research, Department of Energy, National Institutes of Health and the Beckman Laser Institute and Medical Clinic Endowment. Supported in part by the Slovenian Ministry of Science and Technology (BM). The authors thank Bruce J Tromberg for an insightful discussion.

References

Anvari B, Milner T E, Tanenbaum B S, Kimel S, Svaasand L O and Nelson J S 1995a Selective cooling of biological tissues for thermally mediated therapeutic procedures *Phys. Med. Biol.* **40** 241–52

Anvari B, Tanenbaum B S, Milner T E, Kimel S, Svaasand L O and Nelson J S 1995b A theoretical study of the thermal response of skin to cryogen spray cooling and pulsed laser irradiation: implications for the treatment of port wine stain birthmarks *Phys. Med. Biol.* **40** 1451–65

Barsky S H, Rosen S, Geer D E and Noe J M 1980 The nature and evolution of port wine stains: a computer-assisted study *J. Invest. Dermatol.* **74** 154–7

Crostack H A, Jahnel W, Meyer E H and Pohl K J 1989 Recent developments in non-destructive testing of coated components *Thin Solid Films* **181** 295–304

Groetsch C W 1984 *The Theory of Tichonov Regularization for Fredholm Equations of the First Kind* (New York: Pitman)

Jacques S L, Nelson J S, Wright W H and Milner T E 1993 Pulsed photothermal radiometry of port-wine-stain lesions *Appl. Opt.* **32** 2439–46

Kelman G R and Nunn J F 1966 Nomograms for correction of blood pO_2, pCO_2, pH, and base excess for time and temperature *J. Appl. Physiol.* **21** 1484–90

Long F H, Anderson R R and Deutch T F 1987 Pulsed photothermal radiometry for depth profiling of layered media *Appl. Phys. Lett.* **51** 2076–8

Lucassen G W, Verkruysse W, Keijzer M and van Gemert M J C 1996 Light distribution in a port wine stain containing multiple cylindrical and curved blood vessels *Lasers Surg. Med.* **18** 345–57

Majaron B, Verkruysse W, Tanenbaum B S, Milner T E and Nelson J S 2000 Pulsed photothermal profiling of hypervascular lesions: some recent advances *Lasers in Surgery: Advanced Characterization, Therapeutics, and Systems X* vol 3907, ed R Anderson *et al* (Bellingham, WA: SPIE) pp 114–25

Milner T E, Goodman D M, Tanenbaum B S and Nelson J S 1995 Depth profiling of laser-heated chromophores in biological tissues by pulsed photothermal radiometry *J. Opt. Soc. Am.* A **12** 1479–88

Milner T E, Smithies D J, Goodman D M, Lau A and Nelson J S 1996 Depth determination of chromophores in human skin by pulsed photothermal radiometry *Appl. Opt.* **35** 3379–85

Prahl S A 1996 Pulsed photothermal radiometry of inhomogeneous tissue *Progress in Photothermal and Photoacoustic Science and Technology Series: Life and Earth Sciences* vol 3, ed A Mandelis and P Hess (Bellingham, WA: SPIE)

Smithies D J, Milner T E, Tanenbaum B S, Goodman D M and Nelson J S 1998 Accuracy of subsurface distributions computed from pulsed photothermal radiometry *Phys. Med. Biol.* **43** 2453–63

Tam A C and Sullivan B 1983 Remote sensing applications of pulsed photothermal radiometry *Appl. Phys. Lett.* **43** 333–5

van Kampen E J and Zijlstra W G 1965 Determination of hemoglobin and its derivatives *Advances in Clinical Chemistry* ed H Sobotka and C P Stewart (New York: Academic) p 158

Verkruysse W, Lucassen G W, de Boer J F, Smithies D J, Nelson J S and van Gemert M J C 1997 Homogeneous versus discrete absorbing structures in turbid media *Phys. Med. Biol.* **42** 51–65

Verkruysse W, Majaron B, Tanenbaum B S and Nelson J S 2000 Optimal cryogen spray cooling parameters for pulsed laser treatment of port wine stains *Lasers Med. Surg.* at press

Verkruysse W, Nilsson A M K, Milner T E, Beek J F, Lucassen G W and van Gemert M J C 1998 Optical absorption of blood depends on temperature during a 0.5 ms laser pulse at 586 nm *Photochem. Photobiol.* **67** 276–81

Verkruysse W, Pickering J W, Beek J F, Keijzer M and van Gemert M J C 1993 Modelling the effect of wavelength on the pulsed dye laser treatment of port wine stains *Appl. Opt.* **32** 393–8

Vitkin I A, Wilson B C and Anderson R R 1995 Analysis of layered scattering materials by pulsed photothermal radiometry—application to photon propagation in tissue *Appl. Opt.* **34** 2973–82

Wan S, Anderson R R and Parrish J A 1981 Analytical modelling for the optical properties of the skin with in vitro and *in vivo* applications *Photochem. Photobiol.* **34** 493–9

Zhao Y, Chen Z, Saxer C E, deBoer J F, Majaron B, Verkruysse W and Nelson J S 2000a Optical Doppler tomography for monitoring laser treatment of port wine stain *Coherence Domain Optical Methods in Biomedical Science and Clinical Applications IV* vol 3915, ed V V Tuchin, J Aizatt and G Fujimoto (Bellingham, WA: SPIE) pp 237–42

Zhao Y, Chen Z, Saxer C E, Shen Q, Xiang S, deBoer J F and Nelson J S 2000b Phase resolved OCT/ODT for monitoring the efficacy of port wine stain laser therapy in situ *Opt. Lett.* at press